CASE STUDIES TO ILLUSTRATE THE ROTORCRAFT CERTIFICATION BY SIMULATION PROCESS; CS 27/29 DYNAMIC STABILITY REQUIREMENTS

Linghai Lu, Cranfield University, Cranfield, United Kingdom
Gareth Padfield, University of Liverpool, Liverpool, UK
Mark White, University of Liverpool, Liverpool, UK
Christopher Dadswell, University of Liverpool, Liverpool, UK
Giuseppe Quaranta, Politecnico di Milano, Milano, Italy
Stefan van't Hoff, Royal Netherlands Aerospace Centre, NLR, Amsterdam, The Netherlands
Philipp Podzus, German Aerospace Center, DLR, Braunschweig, Germany

Abstract

This paper is one of a set presented at the 49th European Rotorcraft Forum displaying results from the EU Clean Sky 2 project, Rotorcraft Certification by Simulation (RoCS). The process developed by the RoCS team provides guidance on the requirements for the use of simulation in certification and features four case studies that illustrate aspects of the process applied using flight simulation models and flight test data provided by Leonardo Helicopters. This paper presents the case study on Dynamic Stability, for the relevant certification paragraphs in the EASA Certification Specifications CS-27 and CS-29. The Dynamic Stability paragraphs from the Specifications are described and results from simulation model fidelity assessment, and updating compared with test data, are presented for a reference flight condition. The credibility of extrapolations of the flight simulation model results to conditions at higher altitude, different airspeeds and vertical rates of climb are then discussed. Preliminary results from piloted simulation trials, with a 'new' flight test manoeuvre, are included to illustrate flight simulator fidelity assessment methods and to explore the veracity of the stability margins set by the Certification Specifications.

List of Symbols

A_η	Control (η) attack = $\frac{\dot{\eta}_{pk}}{\Delta\eta}$
I_{xz}	Product of inertia
M/U	Confidence (Margin/Uncertainty) ratio
N_p,N_r, N_v	Yaw moment stability derivatives
L_p,L_r, L_v	Roll moment stability derivatives
V	Flight airspeed
XA, B, C, P	Pilot controls, lat cyclic, long cyclic, collective, pedal
Y_p,Y_r, Y_v	Sway force stability derivatives
p, q, r	Aircraft roll, pitch and yaw rates
$t_{d(1/2)}$	Time to double (half) amplitude
u_{turb}, v_{turb}, w_{turb}	Turbulence components, Earth axes
α, β	Incidence, sideslip angles
$\dot{\eta}_{pk}$	Peak rate of control deflection
η	Pilot control deflection
$\mu\,(\zeta)$	Mode (relative) damping
λ	Mode eigenvalue
ϕ, θ	Aircraft roll, pitch angles
$\omega\,(\omega_n)$	Mode (natural) frequency

List of Acronyms

AC	Advisory Circular
ACR	Applicable Certification Requirement
ADS-33	Aeronautical Design Standard-33
AR	Attack Activity Rate
c.g.	Centre of Gravity
CR	Confidence Ratio
CS	Certification Specification
DoE	Domain of Extrapolation
DoP	Domain of Prediction
DoR	Domain of Reality

DoV	Domain of Validation
EASA	European Union Aviation Safety Agency
ERF	European Rotorcraft Forum
FAA	Federal Aviation Administration
F-AW109	FLIGHTLAB model of AW109 Trekker
FS	Flight Simulator
FSM	Flight Simulation Model
FTM	Flight Test Manoeuvre
FTMS	Flight Test Measurement System
HQ(R)	Handling Qualities (Rating)
IFR	Instrument Flight Rules
I-P	Influence-Predictability
LDO	Lateral Directional Oscillation
MTE	Mission Task Element
NRC	National Research Council (Canada)
RCbS	Rotorcraft Certification by Simulation
RoCS	Rotorcraft Certification by Simulation
SAS	Stability Augmentation System
VFR	Visual Flight Rules
V&V	Verification and Validation

1. INTRODUCTION

Aircraft are 'certified' before entering service by demonstrating compliance with the safety requirements set by relevant authorities. Both the structure of the certification process and the means to demonstrate compliance must be agreed between the applicant and the authority. The compliance demonstration is usually performed through flight and ground tests, often the lengthiest and most expensive phase of the certification process. Moreover, flight testing can sometimes pose safety risks, e.g. those related to flight control system or engine failures. Other tests must be carried out in special environmental conditions, e.g. at high-density altitude, low/high temperature. The test envelope of potential flight conditions (e.g. airspeed/altitude envelope) and aircraft configurations (e.g. weight and balance) is clearly extensive. To reduce the scope of flight test activities, analysis-based methods of compliance, including flight simulation, are being explored. For instance, Leonardo Helicopters have used simulation in the certification of the engine-off landings for the AW189 (Ref. 1), and tail rotor loss of effectiveness for the AW169 (Ref. 2).

Both EASA's CS-27 and CS-29 Subpart B (Flight) define the term "analysis-based" methods of compliance as "*calculations*" in the clause of *"tests upon a rotorcraft of the type for which certification is requested, or by calculations based on, and equal in accuracy to, the results of testing"* (Refs. 3 and 4). Federal Aviation Administration (FAA) Advisory Circular AC-29.21(a) states that "*calculation*" includes flight simulation (Ref. 5) and the FAA's AC 25-7D §3.1.2.6 defines the general principles under which flight simulation may be proposed as an acceptable alternative to flight testing for large aeroplanes (Ref. 6).

With the improvements in fidelity of physics-based rotorcraft flight simulation models, their use to supplement or replace flight testing through a virtual-engineering process is likely to become more extensive as industry pursues increased efficiency and safety and reduced cost (Ref. 7). The team of the European CleanSky2 funded project, Rotorcraft Certification by Simulation (RoCS, project acronym), is exploring the possibilities and limitations, and developing guidelines for best practices, in the application of flight simulation to demonstrate compliance with the flight-related airworthiness regulations for helicopters and tiltrotors (Ref. 8).

Preliminary Guidelines for the application of (rotorcraft) flight modelling and simulation have been developed in support of certification for compliance with standards CS-27/29, PART B (Flight) and other flight-related aspects (e.g. CS-27/29, Appendix B, Airworthiness Criteria for Helicopter Instrument Flight, Refs. 9 and 10). The Guidelines promote a requirements-based approach in the form of a structured process for Rotorcraft Certification by Simulation (RCbS, process acronym) (Ref. 9). The process starts with the selection of 'applicable certification requirements' (ACRs), with judgements on a matrix of factors of Influence (how the RCbS process will be applied), Predictability (extent of interpolation/extrapolation), and Credibility (level of confidence in results), together with a comprehensive description of flight simulation requirements. Case Studies drawn from selected ACRs are conducted to demonstrate the efficacy of aspects of the process, including the

selection of metrics and tolerances for fidelity sufficiency and credibility analysis.

This paper presents the results from the case study on the Dynamic Stability (DS) ACR, CS 29.181, and CS 27/29 Appendix B, to illustrate the application of the RCbS process. Section 2 summarises the RCbS process; Section 3 describes the range of different requirements for dynamic stability, with a discussion on the implications for handling qualities (HQs) and pilot workload. Section 4 presents the results from the case study, applying the RCbS process to the dynamic stability ACR, including the credibility of extrapolation of the findings to different flight conditions. Section 5 introduces a new flight-test-manoeuvre (FTM), in the style of ADS-33's mission-task-elements (MTEs) (Ref. 11), designed to evaluate the impact of reducing, but still compliant, levels of dynamic stability on pilot workload, including flight in turbulent atmospheric conditions. Results from exploratory piloted simulation trials are presented. Section 6 then summarises the main conclusions and associated recommendations derived from this RoCS case study.

2. GENERAL OVERVIEW OF THE RCbS PROCESS

The Guidance for the RCbS process is organised into three, serial but iterative, phases, as shown in Figure 1 and expanded on in Refs, 9 and 10.

1) Phase 1; requirements-capture and build,
2) Phase 2; developments of flight simulation model (FSM, 2a), flight simulator (FS, 2b) and Flight Test Measurement System (FTMS, 2c);
3) Phase 3; Credibility assessment and Certification.

The activities in these three phases are undertaken within a governance framework defined in the Project Management Plan and created in Phase 0 of the RCbS process.

Phase 1 contains subtasks for a selected ACR – selecting the appropriate Influence and Predictability (I-P) levels, defining the simulation types and critical features, and assembling their detailed requirements. The application of RCbS is contained within different domains as illustrated in Figure 2, for two flight condition parameters, p_1 and p_2.

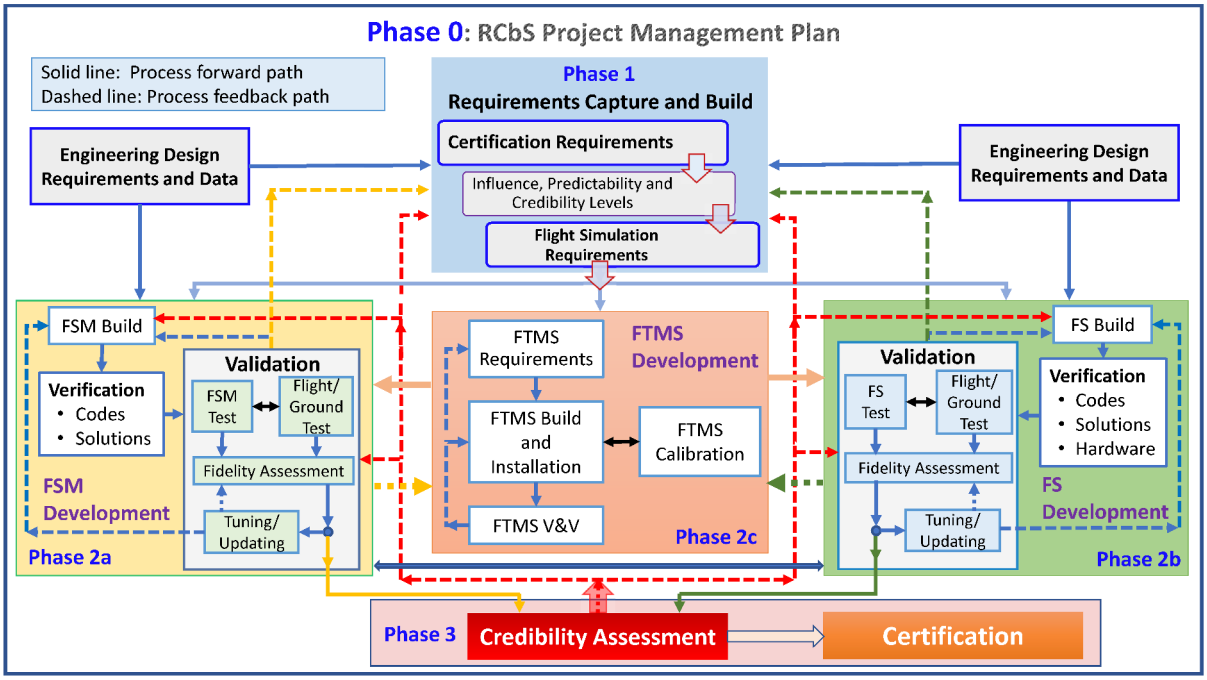

Figure 1: The RCbS process summarised (Refs 9, 10)

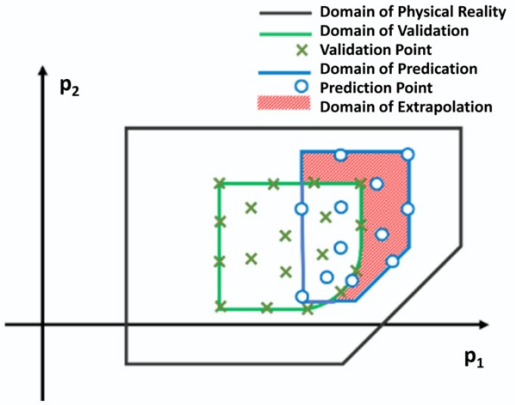

Figure 2: The domains in the RCbS process

In summary,

a) The domain of physical reality (DoR) is the domain within which the laws of physics being used are considered to be adequately represented in the flight model and flight simulator.
b) The domain of prediction (DoP) is the domain within which it is the intention to predict the behaviour of the aircraft and its components and to use these predictions to support certification at the defined I-P Levels.
c) The domain of validation (DoV) is the domain within which test data are used to validate the flight simulation. Interpolation is used in the DoV to predict behaviour between validation points.
d) The domain of extrapolation (DoE) is the domain within which extrapolations of predictions are made to achieve certification at defined Influence Levels for an ACR.

Figure 3 illustrates an example of how the I-P Matrix might be configured, showing the four forms of influence and predictability (i.e. 16 possible combinations). The example ACR is CS 29.181 and CS 27/29 Appendix B, relating to Dynamic Stability, details of which will be given in the next Section. Through interpolation in the DoV, partial credit is being sought for a wide range of flight conditions and aircraft configurations, including, e.g. varying altitude, flight path angle, weight and balance (I3-P1). Then, within the DoE, critical Point analysis is proposed (I2-P4) to down-select a set of flight cases for achieving full credit by extensive extrapolation (I4-P3).

De-risking (I1) can be used at any point in Phase 2, for example as safety-of-flight exercises during the aircraft development.

RCbS ACR	Influence Levels	Predictability Levels			
		Full Interpolation in DoV (P1)	Extensive interpolation in DoV Limited extrapolation in DoE (P2)	Interpolation in DoV Extensive extrapolation in DoE (P3)	Full extrapolation in DoE (P4)
CS 29.181 Dynamic Stability	De-risking (I1)				
	Critical Point Analysis (I2)				
	Partial credit (I3)				
	Full credit (I4)				

Figure 3: Selection of the Influence and Predictability levels in the RCbS process

Figure 4 illustrates how the 'trim' test point matrix might be defined; in this case, nine (forward) flight speeds and five density altitudes. Note that in this hypothetical case the high-altitude hover and high speed cases are considered outside the flight envelope. At each of these 43 test conditions could be added variations in flight path angle (vertical and horizontal) and turn rate, acknowledging the changing behaviour of the aircraft in, e.g. climbing, sideslipping or turning flight. Adding a positive and negative increment for each variable (e.g. ±1000ft/min vertical rate, ±10deg sideslip, ±9deg/sec turn rate) trebles the number of test conditions at each trim point, giving a possible total of 1161 test points. The flight conditions are accompanied in Figure 4 by nine possible aircraft weight (low, mid, height) and longitudinal balance (forward, mid, aft centre of gravity (c.g.)) configurations, giving an accumulated total of 10449 points. A comprehensive assessment of dynamic stability across this hypothetical forward-flight envelope might involve several hundred hours of testing and, depending on the productivity, months of elapsed time. Recalling that this is for a single ACR, it is obvious that this level of coverage is unlikely to be achieved in flight test. Indeed, current certification practice does not require establishing stability sensitivity to variables such as flightpath and turn rate. In comparison, depending on the computer power available and FSM complexity, the dynamic (and static) stability results and analyses can be 'crunched' and documented within a few hours, or days at the most.

To make the assessment more realistic, Figure 4 shows the test points identified as either flight tested, interpolated-simulation in the DoV or extrapolated-simulation in the DoE. With the low-medium altitude cases bookended by flight test, and the high-altitude cases bookended by the high weight, fore and aft c.g. aircraft configurations, this arrangement gives a 62% replacement of flight test by simulation.

Of course, this form of productivity metric is only one aspect of the benefits of RCbS, but it gives a flavour of the potential. All the above are defined (and agreed on) in Phase 1 of the RCbS process, including metrics and tolerances for fidelity to be used in Phase 2 and the uncertainty analysis and credibility metrics in Phase 3. The extensive activities in Phase 2 describe how the FSM/FS/FTMS developments meet the requirements, including Verification and Validation (V&V), fidelity assessment and any required physics-based model updating. Based on the successful achievements in Phase 2, Phase 3 can then focus on extrapolation, credibility assessment and certification.

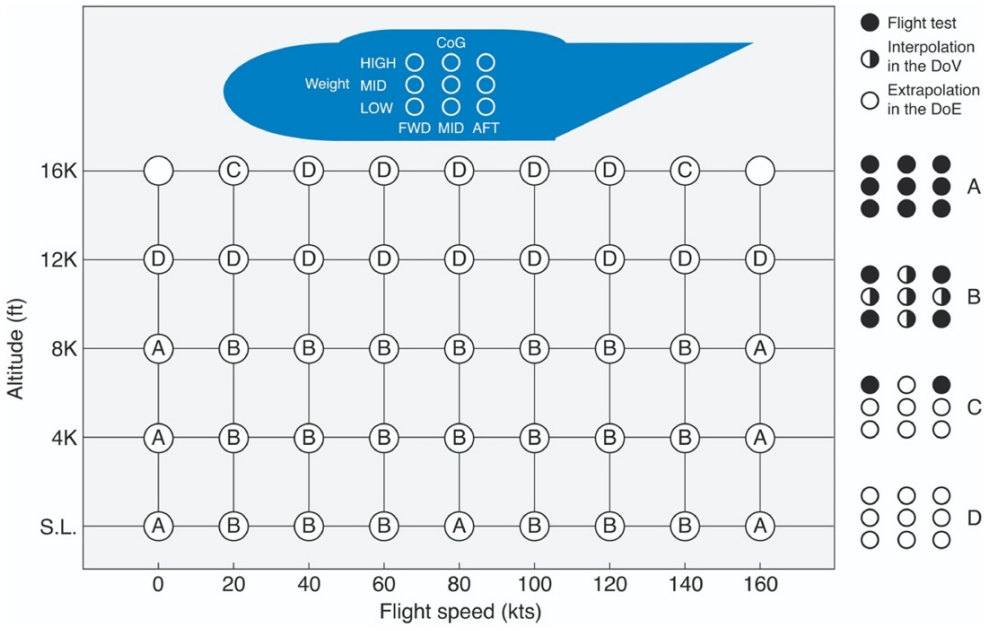

Figure 4: Possible matrix of test points for an ACR

In the next section, the RoCS dynamic stability case study is presented in detail, set within a brief historical context. The authors recognise that an assessment of static stability ACRs would likely accompany those for dynamic stability; results from the former used to support the latter. In the present exercise, only dynamic stability is considered.

3 DYNAMIC STABILITY AS A FLYING QUALITY

The relevant CS-29 certification requirement is CS-29.181 (Dynamic Stability). For small rotorcraft, CS-27.171 states that for flight under Visual Flight Rules (VFR), "*the rotorcraft must be able to be flown, without undue pilot fatigue or strain, in any normal manoeuvre for a period of time as long as that expected in normal operation.*" The descriptors 'undue' and 'normal' are not elaborated on in the specifications. For flight under instrument flight rules (IFR), as presented in CS 27/29 Appendix B, the requirements are quantified in terms of how much the motion must damp within various oscillation cycles. So, for example, for single-pilot IFR, CS-27 requires that, "*any oscillation having a period of less than 5 seconds must damp to ½ amplitude in not more than one cycle*." This requirement also applies to CS-29 IFR operations. Such 'flying quality' requirements can be shown on a chart of oscillation frequency vs damping. Figure 5 shows the chart with multiple boundary lines for dynamic stability that can be related to the various flight 'modes', e.g. pitch-heave short-period, phugoid or lateral-directional Dutch-roll.

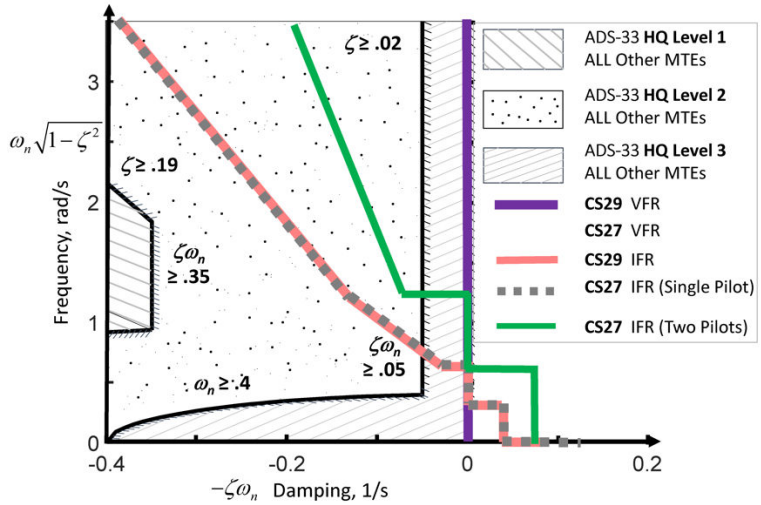

Figure 5: Boundaries of acceptable dynamic stability on a chart of frequency (rad/sec) vs damping (1/sec)

In flight dynamics modelling parlance, each mode has an associated eigenvalue (λ), that can be derived from the linearised form of the FSM,

(1) $$\lambda = \mu \pm i\omega$$

where the real part, μ, is the mode damping and the imaginary part, ω, is the mode frequency. The exponential way that such modes grow or decay to double or half amplitude, is inversely proportional to the magnitude of the damping, i.e.

(2) $$t_d\,(t_{1/2}) = 0.69/|\mu|$$

The relative damping, or damping ratio, (ζ), quantifies how many oscillation cycles a mode grows or decays to double or half amplitude ($N_{1/2}$), i.e.

(3) $$N_{1/2} = \frac{0.69}{2\pi}\frac{\sqrt{1-\zeta^2}}{\zeta}$$

The mode damping and frequency are related to the relative damping (ζ) and the (undamped) natural frequency (ω_n) through the equations,

(4) $$\mu = \zeta\,\omega_n$$

(5) $$\omega = \omega_n\sqrt{1-\zeta^2}$$

The diagonal boundaries in Figure 5 are lines of constant damping ratio, reflecting that the higher the mode frequency, the larger must be the damping for acceptable flying qualities. The higher the frequency of disturbed motions, the quicker pilots must work to suppress deviations in flight path or attitude. So, the CS-27 single pilot IFR line referred to earlier corresponds to a ζ of about 0.11, or 11% of critical damping. The two-pilot (green) line corresponds to a lower ζ value of about 0.055. From Figure 5, at low frequency, some instability is allowed; specifically, for single pilot IFR (grey-dashed line):

a) *Any oscillation having a period of 20secs or more may not achieve double amplitude in*

less than 20secs.

b) *Any aperiodic response may not achieve double amplitude in less than 6secs.*

Figure 5 also includes the ADS-33E HQ Level boundaries for minimum acceptable flying qualities for lateral-directional oscillations (LDO) in forward flight for the so-called 'all other MTEs' category (Ref. 11). Not shown on the figure, for tracking and target-acquisition MTEs, a minimum value of ζ=0.35 is required for Level 1 flying qualities, to ensure a high level of precision can be achieved with minimal pilot compensation. The Level 1-2 boundary for the all-other-MTEs category sits at a relative damping of about 0.19, above a frequency of about 1.8rad/sec. The ADS-33 boundaries at lower frequencies are more complex as shown in Figure 5, partly to harmonise with other flying qualities requirements. To achieve the Level 1 standards, ADS-33 also sets metrics for the ratio and phase of roll to sideslip/yaw in the LDO (Ref. 12). The civil specifications make no reference to HQ Levels; for each category, there is a single boundary discriminating acceptable from unacceptable behaviour.

The relative damping standard format was first applied in the 1950s for the military helicopter standard, MIL-H-8501 (Ref. 13) and has been adopted with minimal modification in both US and European civil certification specifications. They also feature in the fixed-wing specification (Ref. 14). The higher the mode frequencies, the more likely pilots will need to get 'into-the-loop' to suppress unwanted roll-yaw oscillations, particularly when manoeuvring in turbulent conditions. In Ref. 15, the historical context to this form of flying qualities standard is described and results from FSM fidelity assessment are presented based on flight tests with the National Research Council of Canada's Bell 412 and Liverpool's FLIGHTLAB F-B412 FSM. The LDO stability and response fidelity metrics showed good matches between flight and simulation following a model-update process involving enhanced interference modelling.

While the civil standards in Figure 5 are applicable to any oscillation, this paper also focuses on the LDO. Without stability augmentation, the LDO frequency and damping, for mid-high speed flight conditions, typically lie in the middle of the Figure 5 chart, with frequencies below 2.5rad/sec. The means to establish compliance with the dynamic stability requirements of CS-27/29 involves the pilot setting up the appropriate trim condition, applying a pedal doublet and allowing the roll-yaw-sideslip oscillations to respond freely for several cycles. The frequency and damping can then be computed from the time responses; the ADS-33 test guide (Ref. 16) describes how this can be achieved in detail. ADS-33 notes that "*if the oscillation is nonlinear with amplitude, the requirement should apply to each cycle of oscillation*." The civil standards do not specifically address this point. However, because of the nature of fuselage/empennage force and moment variations with sideslip, such nonlinear behaviour is likely be a normal situation. In the present case study, the variations with amplitude are contained within uncertainty analyses, as described later in this paper.

The absence of supporting data for the CS boundaries in Figure 5 raises questions about their veracity. Rotorcraft fitted with a stability augmentation system (SAS) typically feature LDO characteristics well to the left of the boundary lines on the chart. So-called bare-airframe LDO characteristics are more likely to lie in the regions around the boundaries.

To add more depth to the assessment of dynamic stability, an FTM has been designed by the RoCS team and evaluated as part of the dynamic stability case study; preliminary results from piloted simulation trials are presented in Section 5 of this paper.

4 THE LDO IN THE DOMAINS OF VALIDATION AND EXTRAPOLATION

4.1 Test aircraft and flight simulation environment

The RoCS project was provided with flight test data and a FLIGHTLAB FSM of the AW109 Trekker aircraft with which to exercise aspects of the RCbS process, including the case studies reported in the papers presented at this 49th ERF. Bare-airframe[1] flight data for trims, stability and response assessment were provided to the RoCS team, by Leonardo Helicopters, for a range of test conditions, prior to any FSM analysis. Note that in the formal RCbS process, the flight test data would be gathered in Phase 2, in conjunction with the development of the FSM and FS

[1] *In the RCbS process, fidelity assessment for the unstabilised, bare-airframe, configuration is advocated to ensure that the physical sources of fidelity deficiencies can be more clearly determined and, if necessary, corrected.*

and following the development (incl. V&V) of the flight test measurement system (FTMS). Correlations between test and simulation ranged across the quality spectrum. A comprehensive application of the RCbS process would include behavioural fidelity and credibility assessments for the selected ACRs, including any required FSM/FS updating and uncertainty quantification. The RoCS project resources allowed only limited coverage of these aspects, adequate to illustrate the process but not always adequate to establish sufficient fidelity or credibility.

Figure 6 illustrates the component-content of the nonlinear FLIGHTLAB model, the F-AW109. Some key features are the blade-element main rotor with nonlinear lift/drag variations with incidence and Mach number, finite-state dynamic inflow, wake interference and nonlinear fuselage and empennage aerodynamic data derived from wind tunnel tests. The F-AW109 has more than 60 states, including from main rotor flap and lag motions, dynamic inflow, engine and rotorspeed dynamics and control actuators, in addition to those from the six body-motion degrees of freedom.

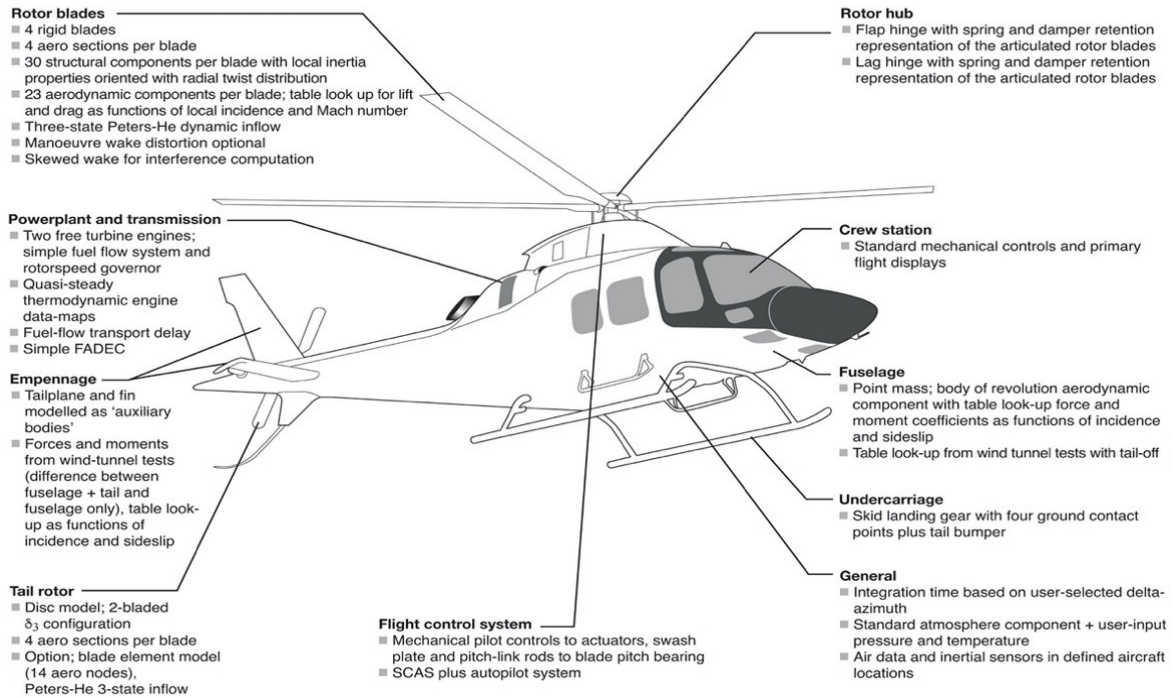

Figure 6: The components of the F-AW109 FSM

In the following, the flight test condition - airspeed 120kts, level at 3000ft density altitude - features as the reference point in the DoV about which dynamic stability extrapolations are carried out. The weight and balance parameters correspond to a light-weight, aft c.g. configuration. LDO stability characteristics for all cases described in this paper are summarised in Appendix A.

4.2 Dynamic Stability characteristics at the reference point in the Domain of Validation

Figure 7 shows a comparison of the (bare-airframe) LDO location from simulation (predicted) vs flight test (FT, estimated) at this condition. Both points are derived from the yaw rate response to a pedal doublet, following CS-27/29 and ADS-33 methodologies (Ref. 16). The uncertainty boxes are derived from the computation of the parameters using different time periods in the response (and input amplitudes in the case of the F-AW109). As noted above, nonlinearities are one source of such variability. The flight and simulation points lie either side of the CS-27/29 IFR boundary but have significant damping margin compared with the CS-29 VFR boundary; recall that CS-27 does not quantify frequency-damping for VFR flight. For reference, the predicted (F-AW109) LDO with SAS engaged, at this flight condition, is also shown on the chart, almost reaching the ADS-33 Level 1-2 boundary for the 'all-other-MTEs' category.

In Figure 7, a 10% fidelity box is shown around the FT estimate. The F-AW109 prediction lies just outside the box. The 10% fidelity tolerance on both frequency

and damping is somewhat arbitrary and would need to be justified by the certification applicant (and agreed with the authority) in Phase 1 of the RCbS process. Failure to achieve the defined tolerance requires that the FSM fidelity is improved with a physics-based update. The process of model-updating to improve fidelity received significant attention by the NATO AVT 296 working group (Ref. 17). Among the methods assessed by the group was the 'renovation technique' developed by the first two authors of the present paper, utilising a system identification approach to estimate the stability and control derivatives that have the greatest impact on fidelity metrics and associated 'cost functions' for the flight-simulator match errors (Ref. 18). For the example presented in Ref. 17 (see also Ref. 15), the LDO prediction for the Bell 412 aircraft required multiple delta derivatives, all linked with aerodynamic interference effects on the empennage and tail rotor. The renovation process then transforms the delta derivatives into auxiliary forces and moments for the relevant FSM component. This approach was adopted in Refs. 19 and 20 as part of the assessment of the ADS-33 LDO flying qualities standards.

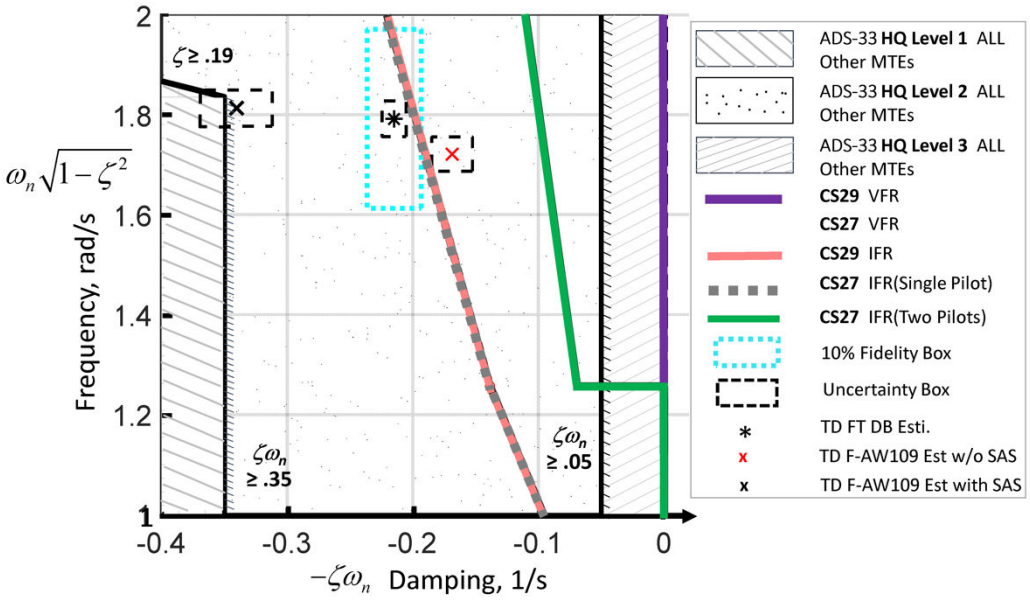

Figure 7: LDO at the DoV reference point (120kts, 3kft; comparison of FSM (x) with flight test (∗))

In the present case, a 10% delta on the yaw damping derivative N_r was sufficient to bring the LDO of the F-AW109 into the fidelity box, as shown in Figure 8. Such a renovation can be linked to minor modifications to parameters in the interference model derived from the finite-state main-rotor inflow model. In such cases, provided the 'tuning' of such parameters is undertaken within the uncertainty ranges, the updating can be considered physics-based. This is clearly a very important aspect of model-updating that applicants need to give detailed attention to.

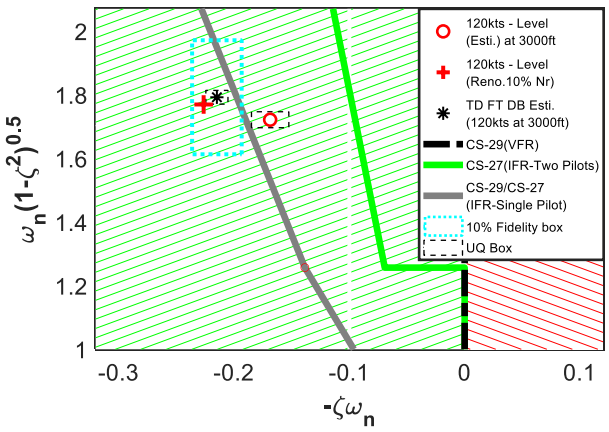

Figure 8: LDO at the DoV reference point (120kts, 3kft) with 10% increase in yaw damping derivative N_r (+)

The large margin of LDO damping for VFR flight might suggest that certification would not be an issue, but the proximity to the IFR boundary might raise concerns for such operations. In Figure 8, the uncertainty effectively negates the small margin. Of course, this is one of the reasons why stability augmentation is commonplace, even for CS-27 rotorcraft.

The 120kts, 3kft altitude flight condition is now used to support extrapolation to a higher altitude condition and, in Sections 4.4 and 4.5, to variations in airspeed and vertical flightpath angle. As part of a 'real' application of the RCbS process, these extrapolations could, for example, be considered in the I3-P2 category (partial credit, limited extrapolation, Figure 3).

4.3 Extrapolation to a higher altitude condition

The results of the application of the 10% increase in yaw damping applied at the extrapolation point, 120kts, 10kft, are shown in Figure 9. The first thing to note is the expected reduction in LDO damping at higher altitude, a consequence of the reduced air density. As an illustration of the accuracy level of this extrapolation, the flight test point for this condition is also shown in the figure, along with corresponding uncertainty and fidelity boxes. Although the damping renovation has brought the LDO prediction into the 10% fidelity box (which would be unknown in a real extrapolation case of course), it appears that the frequency is also under-predicted. Additional renovation, e.g. with the weathercock stability derivative N_v, might be required; the physics of both yaw derivatives are connected of course, through aerodynamic interference effects at the empennage and tail rotor. The example also highlights that extrapolations should normally be derived from more than one point in the DoV, showing trends in the variations of all aspects of the metric, in this case, frequency and damping. At an even higher altitude, say 15kft density altitude, the trends suggest that 10% renovations in frequency and damping derivatives may not provide a sufficiently high confidence in the LDO prediction, hence credibility.

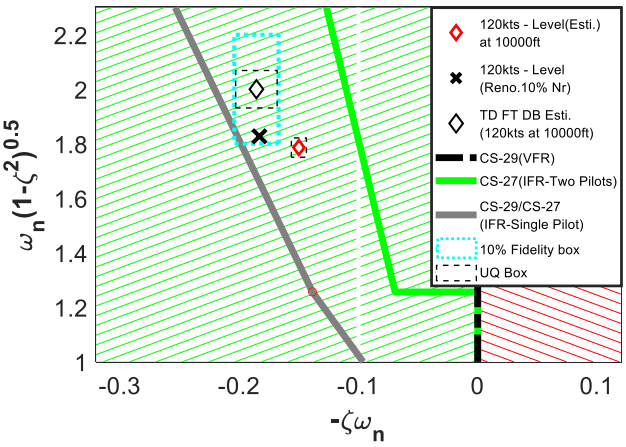

Figure 9: LDO point at the 120kts, 10kft condition with 10% increase in yaw damping derivative $N_r(\mathbf{x})$; flight test estimate shown for comparison

Although it might be expected that the strength of required renovations would vary continuously, even linearly, from the DoV into the DoE, new sources of fidelity deficiency can emerge that require different forms of model structure/form renovation. This example reinforces the importance of establishing the physical basis of the renovation; the physics of the renovation needs to 'keep up' with the reality.

The LDO is particularly sensitive to variations in airspeed and flightpath angle, topics examined in the next two sections.

4.4 Extrapolation to different airspeed conditions

Figure 10 shows how the predicted LDO frequency and damping vary across the airspeed range 100–140kts for the level flight trim condition. Recall that the reference point from the DoV is the 120kts condition. One of the lines in the figure corresponds to the LDO eigenvalues derived from the reduced-order 8x8 state matrix. The FLIGHTLAB linearisation process initially extracts the full state matrix, followed by a model-order reduction process (see for example, Ref. 21) to the selected number of states. This process involves physical assumptions and mathematical approximations, that both need to be validated should the linearised model predictions be used.

The second line in the figure corresponds to the points derived from the yaw-rate oscillations from the nonlinear F-AW109 excited by a pedal doublet, i.e. the standard CS27/29 approach. In both cases the uncertainty boxes are shaped by different amplitude

perturbations or control inputs. The doublet control inputs, with 2sec step duration, ranged up to 10% of maximum pedal. The large uncertainty range for the damping estimation overlaps slightly with the perturbation values for the 140kts flight condition.

The magnitudes of the yaw rate oscillations are only one source of uncertainty relating to the estimation of the LDO characteristics. These represent quantifiable, or epistemic, uncertainties, highlighting that this metric does not represent a unique quantification of dynamic stability; a pilot may find it more, or less, difficult to supress LDO excursions depending on the disturbance amplitude.

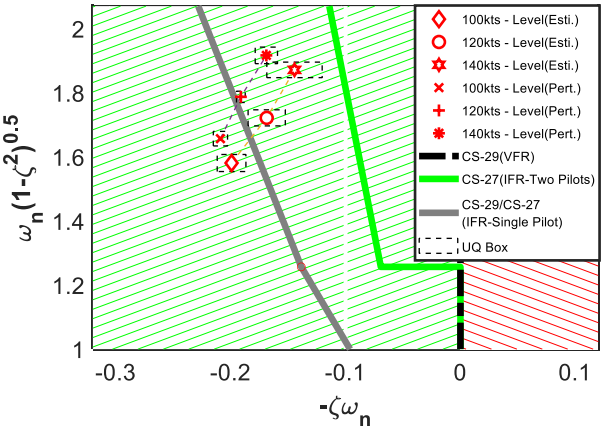

Figure 10: Variation of LDO damping and frequency with airspeed, 100-140kts; comparison of linear system eigenvalue predictions with analysis of F-AW109 yaw rate response to pedal doublet

A key question from this analysis is what is the credibility of these, approximately linear, extrapolations to the different airspeeds? Figure 11 shows the result of renovating the F-AW109 with 10% changes in damping, using the local values of N_r. With only one FT point at 120kts, a DoV trend line cannot be shown of course, but the trend of predictions shows increasing frequency and reducing damping as airspeed increases. Can these trends be explained physically?

One way of exploring the physics behind the changing stability is through the variations in the stability derivatives as a function of airspeed. Figure 12 shows the lateral-directional derivatives varying across the airspeed range under investigation. The weathercock effect N_v) reduces by 20% as airspeed increases from 100-140kts. However, since the LDO frequency is approximately governed by the term $\sqrt{V\ N_v}$, where V is the airspeed, the overall impact is for the LDO frequency to increase with airspeed, consistent with the results in Figure 11. The primary damping contributions are from the derivatives Y_v and N_r, both of which increase by about 25% as airspeed increases across the range, a consequence of the increasing dynamic pressure. The reducing damping evident in Figure 11 has been attributed (Ref. 22) to the impact of the dihedral effect, L_v, that couples with the adverse yaw N_p, when roll and yaw are out-of-phase in the LDO, to give an effective yaw damping,

$$N_{r(eff)} = N_r + N_p \frac{V L_v}{L_p^2} \quad (6)$$

The magnitude of the dihedral effect, largely from the main rotor and fin, increases by about 30% over the airspeed range. The relatively high value of adverse yaw, N_p, constant over the speed range of interest, is due to the roll-yaw coupling effects from the product-of-inertia I_{xz}.

Such effective derivatives, capturing coupling effects, can provide useful physical insight but are far from the whole story (see also Ref. 15). In the present case, coupling with pitch/heave dynamics also plays a part in shaping the LDO, making it very difficult to provide a complete characterisation of behaviour using such approximants.

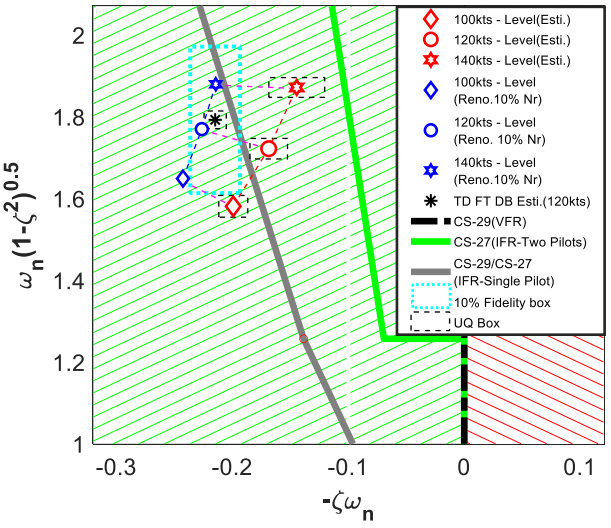

Figure 11: The extrapolated LDOs with 10% renovations in damping (N_r) for 100kts, 120kts, and 140kts conditions

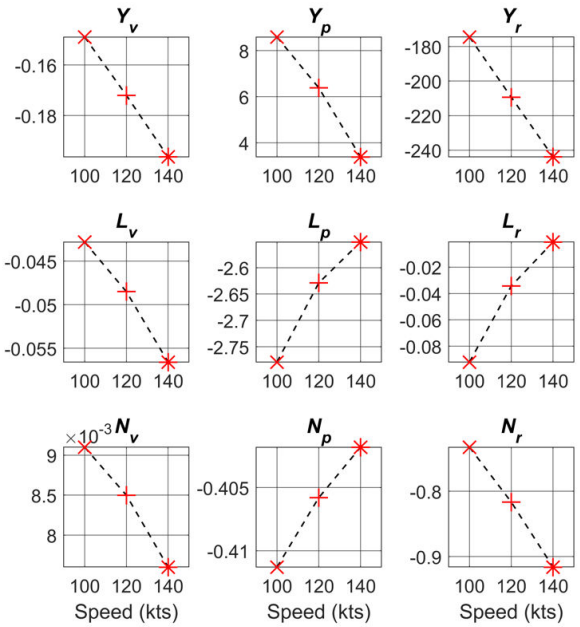

Figure 12: Variations in F-AW109 lateral-directional stability derivatives as a function of airspeed

Small perturbation, 6 degree-of-freedom, derivative-based models can be a valuable source of understanding the behaviour of aircraft, but their limitations should be recognised. Both the amplitude and frequency ranges over which they approximate the dynamics of the nonlinear, multi-state, system are limited and should be assessed before their credibility can be determined. Nonlinear aerodynamics, on the fuselage and empennage particularly, and couplings with higher-order modes, shape these limitations. But such degrading dynamic (LDO) stability, along with improving static and spiral mode stability, are effects that feature in both rotary and fixed-wing aircraft classical flight mechanics. One significant difference is that fixed-wing aircraft rarely fly with negative incidence (α), while this is normal for helicopters in cruise. A consequence is that a perturbation in roll (ϕ) results in an adverse sideslip $V\alpha\phi$, when α is negative (Ref. 21). This has a particularly adverse consequence in climbing flight.

4.5 Extrapolation to different vertical flightpath conditions

As an illustration of the impact of flightpath angle on LDO stability, the composite Figure 13 shows results from flight tests on the research Puma (Ref. 22) in descent, level and climb conditions at 100kts airspeed. The loss of stability as the flightpath angle changes from approximately 6deg descent, through level to 6deg climb is striking. The roll/yaw ratio varies from less than one to greater than 2, one consequence of the adverse sideslip effect described above. These results are for the bare-airframe Puma and contrast with the significantly increased stability provided by the stability and control augmentation system.

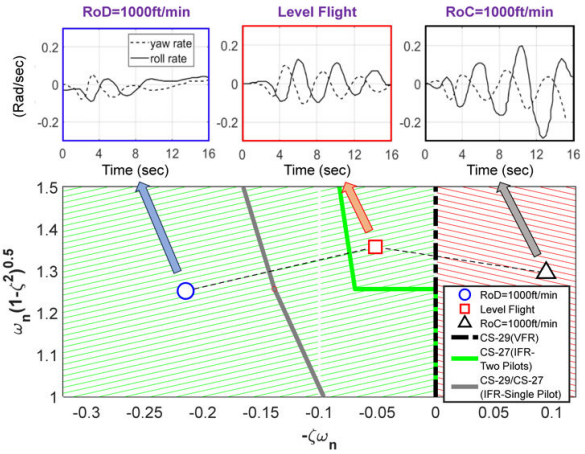

Figure 13: Flight test results from RAE research Puma (SA330) showing variations of LDO stability, and roll/yaw responses to pedal doublet, with vertical flight path, 100kts airspeed (Refs. 21, 22)

Figure 14 shows results from the F-AW109 (bare airframe) pedal doublet analysis, again centred around the 120kts level flight condition. Flight test data in climbing/descending conditions were not available to the RoCS team, so these conditions are firmly in the DoE as presented here. Based on the physical reasoning concerning the negative impact of L_v, the (50%) loss of stability in the climb is expected, and the magnitude of this loss is credible. The aircraft trim pitch angle/incidence varies from -1.5deg to -4deg from the descent to climb condition.

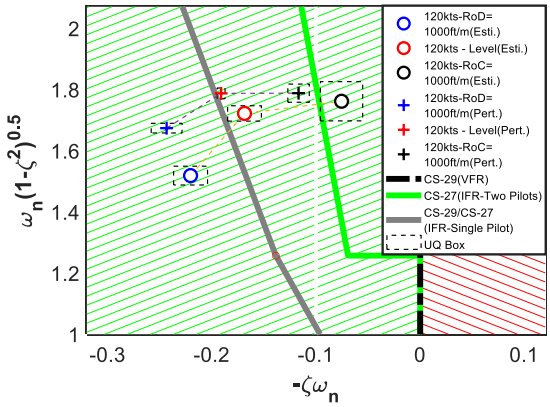

Figure 14: Variation of F-AW109 LDO damping and frequency with vertical rate at 120kts airspeed, -1000ft/min, level, +1000ft/min

Figure 15 shows the impact of the 10% N_r renovations that proved successful for the DoV level flight reference case. The model update increases the stability as expected, but before high confidence in the results can be claimed, the physical sources of the updates should be explained. The increase in the dihedral, L_v, and consequential increase in the LDO roll content are the primary sources for the damping reduction in the climb case. The results from Figure 13 indicate that the HQ degradation might be expected to be larger. If comparative results from other types are used to support or challenge the credibility then, clearly, predictions from the comparative results are an important part of the investigation.

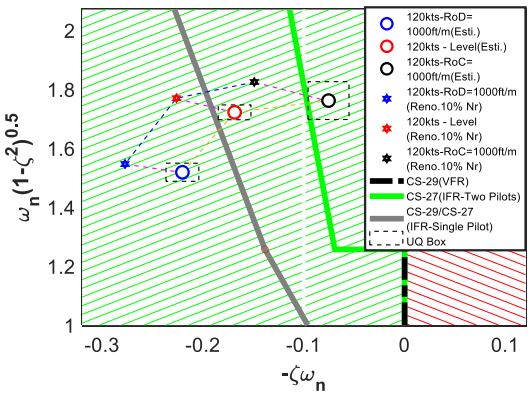

Figure 15: Variation of F-AW109 LDO damping and frequency with vertical rate at 120kts airspeed, -1000ft/min, level, +1000ft/min, with 10% renovations in damping (N_r)

4.6 Credibility in Extrapolation; a discussion

Credibility relates, on the one hand, to the level of understanding that the modeller has in the results of their predictions and, on the other, to the confidence in the level of uncertainty in both the model and test results. Uncertainty analysis goes beyond traditional modelling and simulation perspectives, that tend to focus on model form and parameter accuracy, and rather draws on aspects like statistical variability in design parameters and measurement 'process noise'. Also, the processes of solution and code verification are firmly part of RCbS Phase 2, but outstanding uncertainties can prevail, particularly in time-constrained real-time operation of the FSM in piloted simulation. Being aware of, and able to quantify, uncertainty is recognised as a significant challenge, and the closer the model predictions are to a performance limit/boundary, the more important it becomes to have a measure of uncertainty to support credibility. The RCbS Guidance (Refs. 9, 10) advocates the confidence ratio (CR) concept, M/U; in general terms, the smaller the margin (M) to the limit, the smaller should be the uncertainty (U) to ensure sufficient confidence in the trust of predictions. In the dynamic stability ACR, the margin relates to the level of relative damping (ζ), for the LDO. Taking the CS-27 (2-pilot) IFR boundary in Figures 14 and 15, the renovated model prediction in the climb condition has a small positive 'stability' margin, but the uncertainty box overlaps the boundary. The CR for this case would be very small, likely spoiling the credibility of the prediction.

The LDO stability margin is only one of the metrics in the so-called predicted handling qualities (PHQs) set of ADS-33. While the minimum relative damping for the 'all-other-MTEs' category is 0.19, requirement criteria for attitude bandwidth, quickness and control power as well as multiple cross-coupling metrics must be met for an aircraft to be deemed Level 1; metric ranges also characterise Level 2 or Level 3 HQs. No such metrics feature in CS27/29 but requirements are rather expressed in qualitative terms related to 'controllability and manoeuvrability'. Within the RCbS process, the PHQ metrics are suggested as appropriate measures for the assessment of FSM fidelity, and provide expectations of results in the DoE. They can also be used as sources of evidence for HQ deficiencies that might be 'discovered' in flight test or simulation. The RCbS process therefore recommends the design and conduct of FTMs, in the style of ADS-33 MTEs, as part of the fidelity and credibility assessments and ultimately, if agreed/required, in the certification phase. Such FTMs, with their performance and workload standards, and emphasis on identifying HQ deficiencies, complement the offline predictions, and, where applicable, can replace flight test. The next section describes preliminary results from the exercising of a new FTM for the dynamic stability ACR.

5 PILOTED SIMULATION ASSESSMENT OF THE IMPACT OF THE LDO ON HANDLING QUALITIES

The 45T (45deg turn) VFR FTM is described in Appendix C in the typical MTE format. The pilot is required to fly at 500ft above ground, following a northerly track at 120kts airspeed, then make a 45deg

track change to re-trim. After the turn, the pilot is required to re-establish a zero-bank condition using pedal and cyclic to maintain flight along the new ground-track. The task can be flown in level, climbing or descending flight. The presence of an initial headwind and turbulence are intended to make the task more difficult, increasing the excitation of oscillatory modes like the LDO and highlighting any handling deficiencies (e.g. insufficient stability) to the pilot. The turbulence model was based on the von-Karman power-spectral-density approach (Ref. 23), implemented in the form described in Ref. 24 (p. 678).

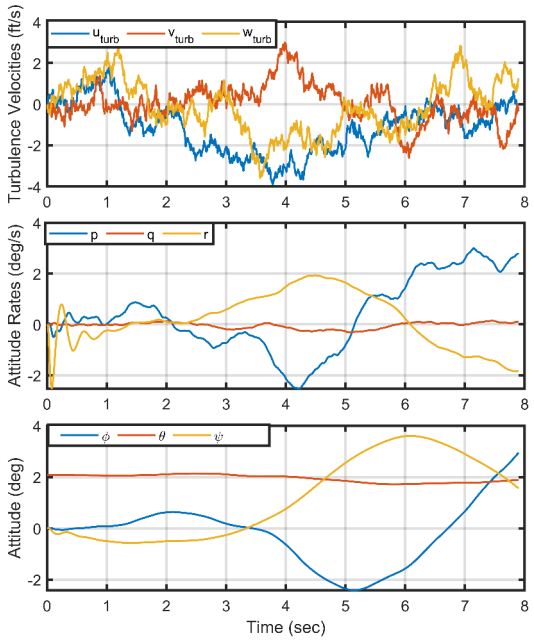

Figure 16: Wind/Earth-axes turbulence components and aircraft responses

Figure 16 shows an 8sec slice of the turbulence components (u_{turb} in the initial headwind (north direction), v_{turb} from west and w_{turb} from below). The aircraft angular rates, that stimulate the inner-ear vestibular sensors, contain components of the higher frequency content, but these are mostly filtered out in the attitude responses.

As noted in Ref. 21, the Gaussian properties of such a turbulence model do not feature the intermittent features more characteristic of structured atmospheric disturbances common in low-level helicopter flight. The statistical-discrete-gust method is proposed in Ref. 21 for such cases, and further investigations with this approach are recommended for application within the RCbS process.

As with the companion RoCS FTMs, the CAT-A rejected-take-off and X-wind hover for controllability and manoeuvrability, full details of the results will be presented in the trial report (Ref. 25).

5.1 Preliminary Test Results

Two test pilots participated in the 'work-up' trials, to support the 'tuning' of the motion drive laws and turbulence model and refining the content of the visual database. Three different test pilots then participated in the RCbS exercise trial with the HELIFLIGHT-R facility (see Appendix B) at Liverpool in July 2023 (Ref. 25). The HQR results from the work-up and exercise trials are presented in Figure 17.

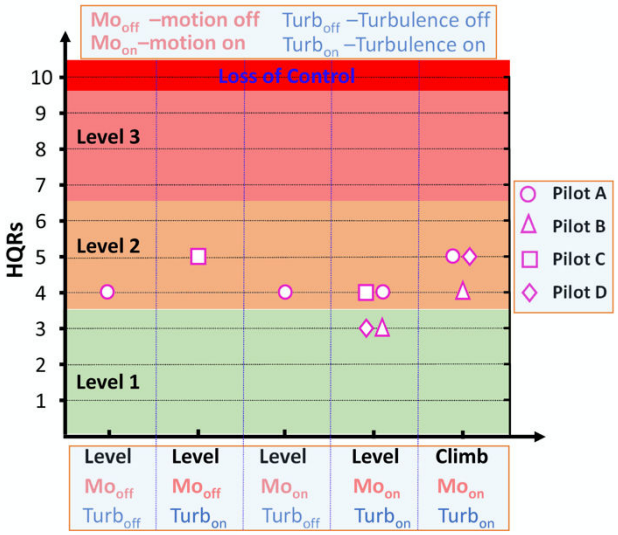

Figure 17: Handling Qualities Ratings for the evaluation pilots flying the 45T at 120kts

During work-up, and with the initial default motion drive algorithm settings, Pilot C experienced adverse (vestibular) motion cues, particularly abrupt proverse yaw cues during the turn-in and turn-out manoeuvres, returning an HQR 7 for inability to maintain the adequate roll angle standards (±7.5deg) during the tracking phase. With the tuned roll-yaw gains and washout parameters, Pilot C achieved the desired standards but with moderate compensation in roll control during tracking (HQR 4). Pilot C also found the vestibular cues improved his ability to perform the 45T compared with the no-motion case (HQR 5).

During the exercise trial, both Pilot B and D rated the reference case as Level 1 (HQR 3), down-rating the climb case to Level 2; Pilot D experienced difficulty holding the climb rate and maintaining the roll angle

in the presence of the weakly damped LDO (HQR 5). Pilot A noted that both vertical and horizontal flight path control were achieved through cyclic with minimal activity on the pedals and collective. In contrast, Pilot B used all four controls continuously throughout the FTM.

Figures 18 and 19 provide 'snapshots' of the kind of results obtained during the trial; here pilot B is flying the rated-runs at the reference condition (HQR 4) and climb condition (HQR 5).

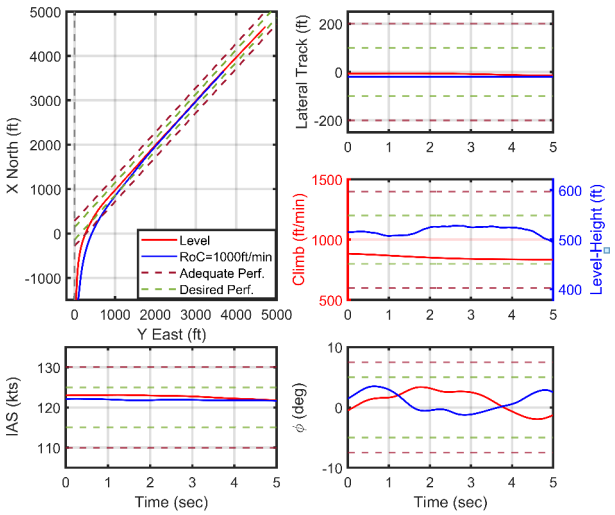

Figure 18: Task performance for pilot B flying the 45T; 120kts reference condition/configuration in level (HQR3) and climbing (HQR4) flight

Figure 18 shows the ground track through the FTM and task performance parameters during the 5sec tracking phase. The LDO, with a period of around 3.5sec, is clearly present in both attitude and sideslip variations (Figure 19), but the pilot is unable to suppress this motion fully. The desired performance is achieved in both cases but with increased compensation in the climb case leading to the HQR 4 (Figure 18). The lateral cyclic, used for adjusting horizontal flight path and roll angle, features a moderate frequency (≈ 4 rad/sec) superimposed on the lower frequency manoeuvre demands, throughout the FTM. The pilot is applying even higher frequency longitudinal cyclic movements, presumably partly in response to the vertical component of turbulence, to maintain the desired airspeed and height/height rate.

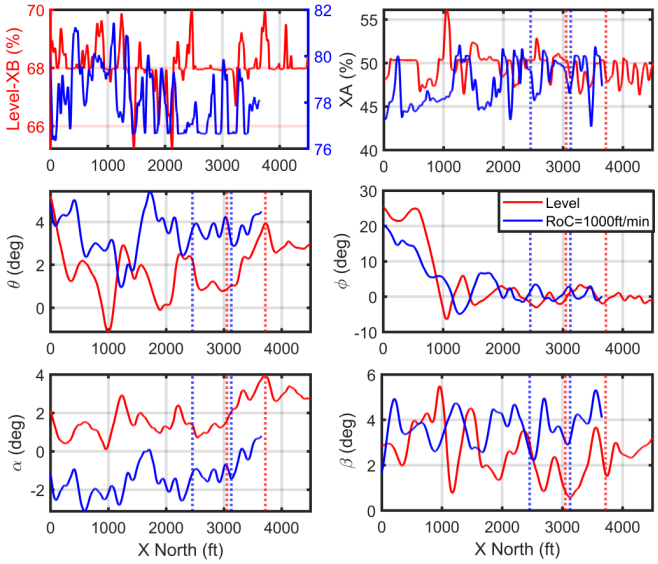

Figure 19: Control activity and attitude/incidence variations for pilot B flying the 45T; 120kts reference condition/configuration in level and climbing flight

A parameter that has proven useful for quantifying control compensation (for handling qualities analysis) and adaptation (for simulator fidelity analysis), is the 'attack' activity rate, based on the control attack metric (A_η), the ratio of peak rate of control deflection, $\dot{\eta}_{pk}$, to amplitude change $\Delta\eta$ (Ref. 21).

$$A_\eta = \frac{\dot{\eta}_{pk}}{\Delta\eta} \tag{7}$$

The number of attacks/sec is then an activity metric as described more fully in Refs. 26 and 27. Fig. 20 illustrates the activity-rate (AR) for pilot B's use of all four controls, derived from 5sec windows through the FTM. While general rules for relating the AR with HQRs are yet to be established, the cyclic peak values between 1 and 2 are consistent with Level 2 ratings in Ref. 26.

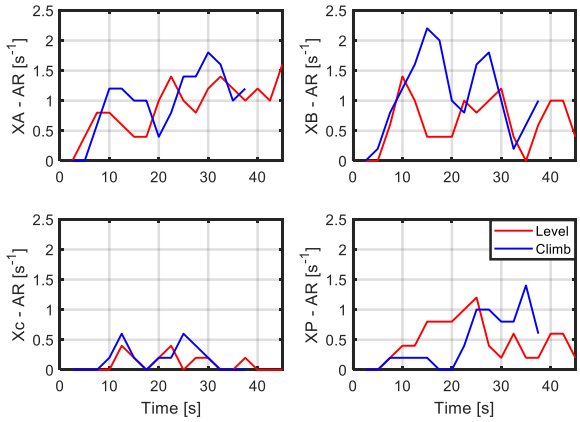

Figure 20: Attack activity rate for all four controls throughout the 45T FTM; pilot B

Combining the AR values from all controls, weighted using relative attack numbers per control (Ref. 26), gives the integrated (peak) AR metric as shown in Fig. 21 plotted on the HQR chart; the individual AR values for the four controls are also shown.

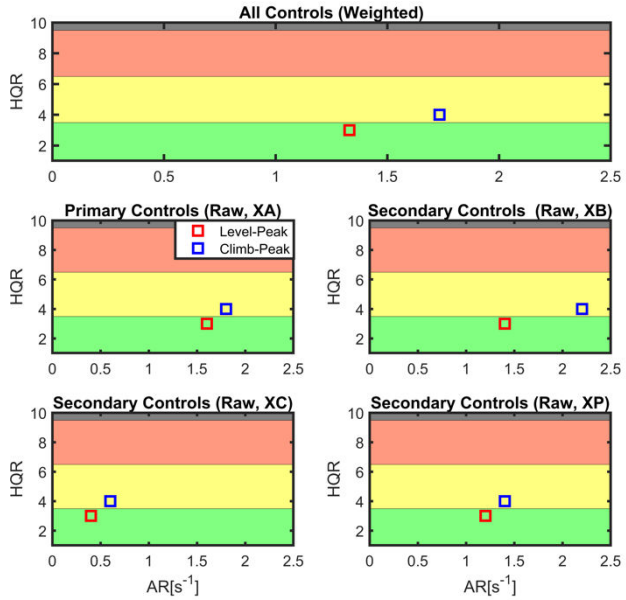

Figure 21: Pilot B's peak attack activity rate for the 45T FTM

The primary control is identified as the lateral cyclic (XA), even though the longitudinal cyclic (XB) features the largest peak values during the entry and exit from the 45deg turn (Fig. 20). The weighted AR increases from about 1.4/sec to 1.7/sec as the level of compensation increases from minimal (HQR 3) to moderate (HQR 4).

In Phase 2 of the RCbS process, it is recommended that control compensation/adaptation metrics such as the attack activity rate are used in concert with the Simulation Fidelity Rating (Ref. 28) scale as part of the predictive/perceptual fidelity assessment.

The Liverpool trial was designed to exercise elements of the RCbS process summarised in Figure 1. To emphasise, the 45T was designed to be part of the fidelity assessment of the flight simulator in Phase 2 of the RCbS process. Without flight test data such fidelity assessment was not possible for this case study.

6 CONCLUDING REMARKS AND RECOMMENDATIONS

This paper has reported on an exercise of the RCbS process and presented of results from the case study on the Dynamic Stability ACR, as expressed in the EASA certification specifications CS27 and CS29. The standards have endured for decades, and while the activity is not intended to challenge the veracity of the standards themselves, it was inevitable that questions would emerge during the study and relevant aspects have been discussed accordingly.

While it is acknowledged that most CS27/29 aircraft feature some form of stability augmentation, the RCbS process has been exercised here on the bare airframe (AW109 Trekker) configuration, to draw out the physical sources of flight behaviour, a strongly recommended element of the process. The RoCS team were provided with flight test data for the bare airframe configuration of the AW-109 Trekker.

A general conclusion from this case study is that dynamic stability can vary considerably from 'normal' straight and level flight conditions examined in the means of compliance assessment. With sufficient fidelity, simulation provides the vehicle for assessment outside this normal. When such assessment is based on extrapolation, fidelity sufficiency should be quantified within the domain of validation that encompasses such conditions, e.g. climbing/descending, turning, sideslipping flight. It is therefore recommended that such conditions be clearly defined by applicants within the domain of prediction during Phase 1 of the process.

The results of the Dynamic Stability analyses have illustrated how the RCbS process can be exercised for an ACR where specific 'performance' requirements are quantified; in this case for the minimum damping ratio across the frequency range of the LDO mode. In the study, the DoV reference condition, 120kts level at 3000ft, was used to derive a FSM update that provided fidelity sufficiency, based on matching within 10% of flight test data. The update process was then applied to extrapolation cases; higher altitude, lower and higher airspeeds and flightpath angle variations. A limited credibility assessment of these extrapolations was explored using results from linear perturbation theory and associated stability derivatives. Such credibility assessment is recommended as part of the RCbS process.

Detailed conclusions from the case study are as follows.

(i) For the DoV reference condition, renovation in the form of a 10% increase in yaw damping was required to bring the LDO prediction into the fidelity sufficiency range.

(ii) While the stability margin for the aircraft at the reference condition was large for CS27/29 VFR operations and CS27 (IFR 2 pilots), it was much smaller for CS27/29 IFR single pilot operations, with the uncertainty effectively equalling the margin ($M/U \approx 1$, Figure 8).
(iii) Renovation of the LDO predictions at a 10,000ft (extrapolation) point showed that the same 10% update in yaw damping achieved sufficient fidelity. However, a further update to the physics behind the frequency prediction would likely be required to strengthen confidence in extrapolations to even higher altitudes.
(iv) The ±17% airspeed extrapolation case showed near-linear variations in the LDO predictions. Credibility in these predictions was reinforced by considering the physics highlighted within the stability derivatives. It is emphasised that this is only one element, albeit a very important one, of the credibility analysis.
(v) Extrapolations about the reference condition to climbing and descending flight revealed much stronger nonlinearities in the predictions. The damping margin in the climb condition (1000ft/min) reduced below the CS27(2-pilot IFR) boundary, with a large spread in uncertainty stemming from nonlinearities in the pedal response oscillations.
(vi) A flight test manoeuvre was designed to assess the veracity of the CS DS standards and for use in the RCbS Phase 2 FS fidelity assessment. The manoeuvre was flown by 4 pilots in the Liverpool HELIFLIGHT-R flight simulator, where the pilot-returned (largely Level 2) HQRs concur with expectations, based on predicted (ADS-33) handling qualities levels. The results are described as preliminary as further/deeper analysis continues to better understand the control strategies and levels of compensation used, key elements of the simulator fidelity assessment. Such an FTM can be used in RCbS Phase 2, direct comparisons with flight results then used to build the DoV for the flight simulator.

The paper is one of a collection of case studies presented at the 49th ERF, material from which will be included in the final issue of the RoCS project Guidelines for the application of modelling and simulation in rotorcraft certification, scheduled for publication in late 2023. The guidelines, presented in brief in Ref 10, advocate a sustained and systematic application of the RCbS process through the duration of a certification 'project'.

Author contacts:

Linghai Lu l.lu@cranfield.ac.uk
Gareth Padfield gareth.padfield@liverpool.ac.uk
Mark White mark.white@liverpool.ac.uk
Chris Dadswell sgcdadsw@liverpool.ac.uk
Giuseppe Quaranta giuseppe.quaranta@polimi.it
Stefan van 't Hoff Stefan.van.t.hoff@nlr.nl
Philipp Podzus philip.podzus@dlr.de

7 ACKNOWLEDGMENTS

The RoCS Project received funding from the CleanSky2 Joint Undertaking (JU) Framework under the grant agreement N.831969. The JU receives support from the European Union's Horizon 2020 research and innovation programme and the Clean Sky 2 JU members other than the Union. The authors wish to acknowledge the support of M. Labatut, F. Paolucci and H. Sallam of EASA and of A. Ragazzi of Leonardo Helicopter Division. Simulation trials at the University of Liverpool during the 'work-up' phase were supported by test pilots Andy Berryman, Charlie Brown and Mark Prior. In addition, EASA test pilot Hamdy Sallam and Volocopter test pilot Paul Stone participated in the RCbS exercise trial in July 2023. Special thanks to Josie Roscoe for supporting the tuning of the motion drive laws during the work-up trials.

8 REFERENCES

1. R. Bianco-Mengotti, A. Ragazzi, F. Del Grande, G. Cito e A., and Brusa Zappellini, "AW189 Engine-Off-Landing Certification by Simulation," AHS 72nd Annual Forum, West Palm Beach, FL, May 17-19, 2016.
2. A. Ragazzi, R. Bianco-Mengotti, and P. Sabato, "AW169 Loss of Tail Rotor Effectiveness Simulation," 43rd European Rotorcraft Forum, Milano, Italy, September 12 – 15, 2017.
3. anon., "*Certification Specifications and Acceptable Means of Compliance for Small Rotorcraft CS-27*," EASA, 2018.
4. anon., "*Certification Specifications and Acceptable Means of Compliance for Large Rotorcraft CS-29*," EASA, 2018.

5. anon., "*AC 29-2C - Certification of Transport Category Rotorcraft*," FAA, Sept. 2008.
6. anon., "*AC 25-7D Flight Test Guide for Certification of Transport Category Airplanes*," FAA, 2018.
7. Padfield, G.D., "*Rotorcraft Virtual Engineering; Supporting Life-Cycle Engineering through Design and Development, Test and Certification and Operations*," The Aeronautical Journal, Vol. 122, No. 1255, pp. 1475–1495, 2018, DOI: 10.1017/aer.2018.47.
8. Quaranta, G., S. van't Hoff, M. Jones, L. Lu, and M. D. White, "Challenges and Opportunities Offered by Flight Certification of Rotorcraft by Simulation," 47th European Rotorcraft Forum, Glasgow, Scotland, UK September 7-9, 2021.
9. van't Hoff S, Lu L., Padfield G., Podzus P., White M., and Quaranta G., "Preliminary Guidelines for a Requirements-Based Approach to Certification by Simulation for Rotorcraft," 48th European Rotorcraft Forum, Winterthur, September 6-8, 2022.
10. Quaranta ,G., van't Hoff S, Lu L., Padfield G.D., Podzus P., White M., "Employment of Simulation for the Flight Certification of Rotorcraft", 49th Annual Forum of the Vertical Flight Society, West Palm Beach, FL, USA, May 16-18, 2023 **(see also www.rocs-project.org).**
11. anon., ADS-33E, "*Aeronautical Design Standard Performance Specification: Handling Qualities Requirements for Military Rotorcraft*," US Army Aviation Engineering Directorate, Redstone, Alabama, March 2000.
12. Key, D.I., Blanken, C.L., Hoh, R.H., Mitchell, D.G., and Aponso, B.L., "Background Information and User's guide (BIUG) for Handling Qualities Requirements for Military Rotorcraft," U.S. Army Research, Development, and Engineering Command, Special Report RDMR-AD-16-01, December 2015.
13. anon., "Military Specification - General Requirements for Helicopter Flying and Ground Handling Qualities," MIL-H-8501A, 1961, superseding MIL-H-8501.
14. Moorhouse, D.J., and Woodcock, R.J., "Background Information and User Guide for MIL-F-8785C, Military Specification-Flying Qualities of Piloted Airplanes," U.S. Air Force Wright Aeronautical Labs Wright-Patterson AFB OH, 1982.
15. Agarwal, D., Padfield, G.D. et al, Rotorcraft Lateral-Directional Oscillations: The Anatomy of a Nuisance Mode, JOURNAL OF THE AMERICAN HELICOPTER SOCIETY 66, 042009 (2021)
16. Blanken, C.L., et al, Test Guide for ADS-33E PRF, Special Report AMR-AF-08-07, AMRDEC, July 2008
17. anon., Rotorcraft Flight Simulation Model Fidelity Improvement and Assessment, NATO STO TR-AVT-296-UU, final report of NATO AVT 296 Research Task Group, NATO May 2021, ISBN 978-92-837-2334-9
18. L. Lu, G. D. Padfield, M. White, and P. Perfect, "Fidelity Enhancement of a Rotorcraft Simulation Model through System Identification," Aeronautical Journal, Vol. 115, No. 1170, 2011. DOI: 10.1017/S0001924000006102.
19. Cameron, N., Memon, W., White, M.D., Padfield, G.D., Lu, L., Agarwal, D., Appraisal of Handling Qualities Standards for Rotorcraft Lateral-Directional Dynamics, AIAA SciTech Forum (virtual), January 2021.
20. Cameron, N., Padfield, et al 4-D analysis for Rotorcraft Lateral-Directional Dynamics, 47th European Rotorcraft Form, Glasgow, September 2021
21. Padfield, G.D., "Helicopter Flight Dynamics", 3rd Edition, Wiley 2018
22. Padfield, G.D., "Flight testing for performance and flying qualities", Helicopter Aeromechanics, AGARD LS-139, May 1985
23. von Karman, T., Progress in the Statistical Theory of Turbulence: Classical Papers in Statistical Theory, Interscience Publications, New York, 1961
24. anon. Flying qualities of piloted aircraft, MIL-HDBK 1797, US Department of Defense Handbook, December 1997
25. anon., RoCS Liverpool trial report, July 2023 University of Liverpool RoCS TRXXX (in preparation)
26. Memon, W., et al Helicopter Handling Qualities: A study in Pilot Control Compensation, The Aeronautical Journal of the RAeS, Volume 126 / Issue 1295 / January 2022, doi:10.1017/aer.2021.87
27. Memon, W., et al., The Development of a Pilot Control Adaptation Metric for Simulation Perceptual Fidelity Assessment, 47th European Rotorcraft Forum, Glasgow, Scotland, Sept 2021

28. Perfect, P., Timson, E., White, M., Padfield, G.D., Erdos, R., A Fidelity scale for the subjective assessment of simulation fidelity, The Aeronautical Journal of the RAeS, Vol 118, No. 1206, August 2014
29. White, M.D., Perfect, P, Padfield, G.D., Gubbels, A.W., Berryman A.C., Acceptance Testing and Commissioning of a Flight Simulator for Rotorcraft Simulation Fidelity Research, Proceedings of the Institution of Mechanical Engineers, Part G, Journal of Aerospace Engineering, November 2011

APPENDIX A LDO stability characteristics

(Est – derived from pedal doublet yaw response; Pert. – derived from F-AW109 linearisation)

100kts, Level, 3000ft, Esti.	-0.1993 ± 1.5806i
100kts, Level, 10% of N_r Reno., 3000ft	-0.2427 ± 1.6484i
120kts, RoC = 1000ft/min, Esti.	-0.0755 ± 1.7613i
120kts, RoC = 1000ft/min, Pert.	-0.1168 ± 1.7877i
120kts, Level, 3000ft, Esti. (Reference case)	-0.1687 ±1.7215i
120kts, Level, 3000ft, Pert.	-0.1912 ± 1.7871i
120kts, Level, 10000ft, Esti.	-0.1500 ±1.7864i
120kts, RoD = 1000ft/min, 3000ft, Esti.	-0.2205 ± 1.5183i
120kts, RoD = 1000ft/min, 3000ft, Pert.	-0.2435 ± 1.6734i
120kts, Level, 10% of N_r Reno., 3000ft	-0.2264 ± 1.7694i
120kts, RoC = 1000ft/min, 10% of N_r Reno, 3000ft	-0.1492 ± 1.8243i
120kts, RoD = 1000ft/min, 10% of N_r Reno, 3000ft	-0.2775 ± 1.5460i
120kts, Level, 10% of N_r Reno., 10000ft	-0.1831 ± 1.8277i
120kts, FT 3000ft, Esti.	-0.2149 ± 1.7921i
120kts, FT 10000ft, Esti.	-0.1856 ± 2.0006i
140kts, Level, 3000ft, Esti.	-0.1445 ± 1.8712i
140kts, Level, 10% of N_r Reno., 3000ft	-0.2144 ± 1.8790i
Puma, 80kts, RoC = 1000ft/min, Esti.	0.0949 ± 1.2954i
Puma, 80kts, Level Flight, Esti.	-0.0518 ± 1.3572i
Puma, 80kts, RoD = 1000ft/min, Esti.	-0.2149 ± 1.2522i

APPENDIX B

Liverpool's HELIFLIGHT-R flight simulation facility

Figure B1: Liverpool's HELIFLIGHT-R research simulator (Ref. 31)

Table B1 HELIFLIGHT-R Motion Capability

	Displacement	Velocity	Acceleration
Pitch	−23.3°/25.6°	±34°/s	300°/s^2
Roll	−23.2°	±35°/s	300°/s^2
Yaw	±24.3°	±36°/s	500°/s^2
Heave	±0.39 m	±0.7 m/s	±1.02 g
Surge	−0.46/+0.57 m	±0.7 m/s	±0.71 g
Sway	±0.47 m	±0.5 m/s	±0.71 g

APPENDIX C – the 45T FTM

<table>
<tr><td>Operation</td><td colspan="3">45deg Turn (45T) in VMC</td></tr>
<tr><td>Critical HQs</td><td colspan="3">LDO stability
Attitude bandwidth and quickness, Cross-couplings: pitch/roll, roll/pitch</td></tr>
<tr><td>Objectives</td><td colspan="3">• Assess the suitability of the (LDO) stability margins defined by CS27/29 through piloted simulation assessment
• Check ability to perform flightpath and speed control in a lateral flight path change manoeuvre in the presence of wind and atmospheric turbulence – in level and climbing flight
• Assess utility of FS to extrapolate the level flight results to climbing flight
• Assess the effect of vestibular motion cueing on task performance, control compensation and pilot perception of simulation fidelity</td></tr>
<tr><td>Manoeuvre Description</td><td colspan="3">The aircraft will be trimmed at a cruise airspeed V of 120 KIAS at a height of 500ft above ground (3,000ft density altitude), on a nominal track angle 360, in the presence of a 20kts headwind with 3-dimensional atmospheric turbulence. The trim bank angle should be zero. The pilot will be following a line on the ground and, at a defined point in space, should manoeuvre to change heading (using approximately 30deg angle of bank) to re-establish level flight following a second line on the ground oriented at a track of 045 (right turn RT). Having stabilised on the new track, the pilot should announce ‘stable’ and maintain the flight condition for 5seconds. The FTM time should be about 20-25secs.
To hold the new track angle, the pilot should adjust the cyclic and pedal/sideslip to maintain zero bank angle.
A first extrapolation case is a repeat of above at a pressure altitude of 10000ft.
A second extrapolation case will be flown trimmed in a climb rate of 1000ft/min; the initial conditions should be such that the aircraft reaches the same point in space (500ft agl) at the start of the turn and maintains rate of climb throughout the manoeuvre.</td></tr>
<tr><td>Test Course Description</td><td colspan="3">The manoeuvre starts on Runway 36 with two runways oriented at +/-45deg to it for the left and right turns. The width of the runways (200ft) indicates the limit of the desired lateral track performance, and the limit of the adequate performance is indicated by pylons which are longitudinally spaced at 500ft.
 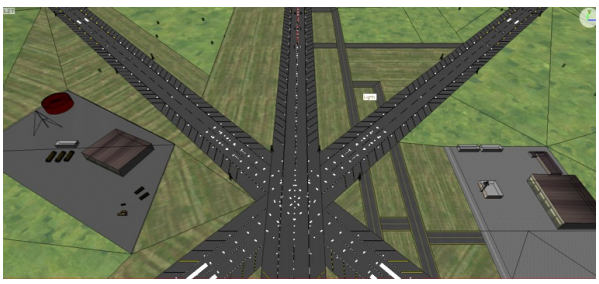 </td></tr>
<tr><td>Ratings Scales</td><td colspan="3">1. Handling Qualities Rating (HQR) Scale
2. Motion Fidelity Rating (MFR) Scale</td></tr>
<tr><td rowspan="5">Performance Standards</td><td></td><td>Desired (d)</td><td>Adequate (a)</td></tr>
<tr><td>Maintain altitude h: or,
Rate of climb (1000ft/min)</td><td>±50ft
±200ft/min</td><td>±100ft
±400ft/min</td></tr>
<tr><td>Maintain airspeed V:</td><td>±5kts</td><td>±10kts</td></tr>
<tr><td>Maintain lateral track after line capture</td><td>± 100ft</td><td>± 200ft</td></tr>
<tr><td>Bank angle during tracking the 45deg runway</td><td>± 5deg</td><td>± 7.5deg</td></tr>
</table>

2023-09-07

Case studies to illustrate the rotorcraft certification by simulation process; CS 29/27 dynamic stability requirements

Lu, Linghai

German Society for Aeronautics and Astronautics (DGLR: Deutsche Gesellschaft für Luft- und Raumfahrt)

Lu L, Padfield G, White M, et al., (2023) Case studies to illustrate the rotorcraft certification by simulation process; CS 29/27 dynamic stability requirements. In: 49th European Rotorcraft Forum (ERF49 2023), 5-7 September 2023, Bückeburg, Germany
https://publikationen.dglr.de/?id=620&tx_dglrpublications_pi1[document_id]=54801023